A Volume-Corrected Kratky Model and the Influence of the Shape of the Orientation Distribution Function on the Molecular Orientation in PPV and Its Precursor

W. Dermaut,[†] T. Van den Kerkhof,[‡] B. Goderis,[§] R. Mertens,[⊥] I. Dolbnya,[#] B. J. van der Veken,[‡] F. Blockhuys,[*,†] and H. J. Geise[†]

Department of Chemistry, University of Antwerp, Universiteitsplein 1, B-2610 Wilrijk, Belgium; Department of Chemistry, University of Antwerp, Groenenborgerlaan 171, B-2020 Antwerpen, Belgium; Department of Chemistry, Katholieke Universiteit Leuven, Celestijnenlaan 200F, B-3001 Heverlee, Belgium; Department of Chemistry, University of Antwerp, Middelheimlaan 1, B-2020 Antwerpen, Belgium; and DUBBLE-CRG/ESRF, Rue des Martyrs 156, B.P. 220, F-38043 Grenoble Cedex, France

Received April 1, 2003; Revised Manuscript Received October 28, 2003

ABSTRACT: The molecular orientation in cold-stretched PPV films was studied with synchrotron WAXD. The results showed that the degree of orientation is comparable to that of hot-stretched films and that it exceeds the latter's orientation for the lower stretch ratios. The values from WAXD and those from previous FTIR dichroic and DECODER NMR measurements are in agreement with each other, but the observed orientation is far higher than predicted by the Kratky model. Therefore, a volume-corrected Kratky model was derived, which takes into account the extra orientation induced by the volume reduction of the polymer during the thermal elimination process. To fully explain the observed orientation values, however, the shape of the orientation distribution function had to be considered as well. It is concluded that this shape should be close to a Gaussian rather than to a Kratky distribution. The orientation in stretch-aligned noneliminated precursor films is discussed as well.

1. Introduction

The possibility of stretch-aligning poly(*p*-phenylenevinylene), PPV, during the conversion at high temperature from precursor to the fully conjugated polymer (see Figure 1 for the structural formulas) was already described in the early reports on the precursor synthesis of this polymer.[1,2] Among others, this stretching improves the conductivity when measured along the stretch direction[3] and increases Young's modulus.[4] Recently, we reported on a new way of producing stretched PPV films: initially the precursor is stretched at low temperature with water vapor as a plasticizer.[5,6] The temperature is raised in a second step with the sample still clamped in the stretching device to create PPV via an elimination reaction. This cold method is experimentally easier than the hot-stretching method and leads to less film tearing and the experimental parameters are much less critical, while a comparable degree of molecular orientation is obtained according to FTIR dichroic measurements. Previously reported data[5] confirm that the molecular orientation is a lot higher than predicted by the existing Kratky model.[2,3,7−9] Recently, the degree of orientation determined with solid-state NMR measurements was reported,[10] and in the present paper wide-angle X-ray diffraction (WAXD) data are added. The combination of the results obtained by these three techniques makes a more elaborate discussion of the molecular orientation possible, and an attempt to explain the deviation from the Kratky model is presented. Finally, the orientation in stretch-aligned precursor films is discussed as well, adding to the understanding of the complex orientation behavior in the PPV films.

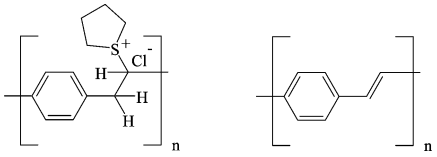

Figure 1. Structure of the precursor polymer (left) and PPV (right).

2. Experimental Section

The experimental procedures concerning the synthesis, sample preparation, stretching procedure, FTIR measurements, and NMR DECODER experiments have been reported earlier.[5,10] X-ray measurements were performed at the DUtch-Belgian BeamLinE (DUBBLE) of the European Synchrotron Radiation Facility (ESRF) in Grenoble, France. A beam with a diameter of 0.8 mm and a wavelength of 1.24 Å was used. The 2D WAXD patterns were recorded on Fuji BAS-III image plates with a sample-to-detector distance of 12 cm. The angles were calibrated using a silicon standard, taking into account the flat film geometry. Thin films of 5 μm were stretched in a homemade stretching device. The exposure time was 5 s. The image plates were digitized with a FUJIX BAS-2000II scanner with a resolution of 100 μm. The result is a 2048 by 2560 matrix image. However, pixels were averaged to a 410 by 512 image, and consequently the resolution was reduced to 500 μm in order to improve the signal-to-noise ratio. Finally, an intensity correction for the use of a flat film and azimuthal readings were made by homemade scripts within the image analysis software V for Windows. The air path length between the sample and the free primary beam appeared to be sufficiently long to generate considerable air scattering. Part of this air scattering was attenuated by the sample up stream, and as a result a shadow of the stretched film could be observed in the images. This hampered a straightforward background correction; i.e., the pattern of an empty sample holder could not be used. To have background-free azimuthal scans through a reflection at a given scattering angle 2θ,

[†] University of Antwerp, Universiteitsplein 1.
[‡] University of Antwerp, Groenenborgerlaan 171.
[§] Katholieke Universiteit Leuven.
[⊥] University of Antwerp, Middelheimlaan 1.
[#] DUBBLE-CRG/ESRF.
[*] Corresponding author: Fax +32.3.820.23.10, e-mail Frank.Blockhuys@ua.ac.be.

10.1021/ma034404y CCC: $27.50
Published on Web 12/13/2003

Table 1. Orientation Values *f* Found for Cold-Stretched and Hot-Stretched PPV Films Using Different Techniques

	cold-stretched PPV			hot-stretched PPV	
stretch ratio	FTIR	WAXD	NMR	FTIR	WAXD
1	0.32		0.38	0.19	
1.5	0.74				
2	0.91	0.942		0.83	0.859
2.5	0.93				
3	0.93	0.975		0.91	0.950
4	0.95	0.975		0.94	0.944
5	0.95	0.983	0.987	0.96	0.955

azimuthal scans were made at a slightly lower 2θ and a slightly higher 2θ value. Care was taken that at the latter two 2θ values no traces of this particular reflection were present or, in other words, that predominantly background is present in these border scans. The background to be subtracted from the 2θ scan containing the reflection of interest was constructed by linear interpolation of the two border scans.

3. Results and Discussion

A. Molecular Orientation in PPV films. a. FTIR Linear Dichroism. The cold-stretched films with a stretch ratio of up to 6 were studied with FTIR dichroic measurements.[5] The analysis from Zbinden[11] was used in order to obtain the so-called Hermans orientation value *f*

$$f = \frac{1}{2}(3\langle\cos^2\gamma\rangle - 1) \tag{1}$$

where γ is the average angle between the chain axis and the stretch direction. When the polymer chains are all perfectly aligned with the stretch direction, *f* will be equal to unity. When all chains are randomly oriented, *f* equals zero. The FTIR-based orientation in both cold-stretched/hot-eliminated and hot-stretched/hot-eliminated PPV can be found in Table 1. It is clearly shown that the orientation rises quickly to very high values, almost attaining its final value at a stretch ratio of 3. The orientation in the cold-stretched/hot-eliminated films of stretch ratios up until three is higher than the corresponding ones in hot-stretched films. This is attributed to the relative ease of orienting a flexible precursor chain as compared to the more difficult orientation of a partly eliminated and hence more rigid PPV domain. Since the orientation in films of higher stretch ratios is very close to perfect, this effect will only be observed at the lower stretch ratios.

b. 2D DECODER NMR. Stacks of several thick (approximately 100 μm) cold-stretched PPV films with a stretch ratio of 5 as well as unstretched films were studied with a 2D solid-state NMR technique called DECODER NMR.[12,13] In this technique, the sample is flipped over a discrete angle with respect to the magnetic field during the measurement. The difference in magnetic environment as experienced by the sample before and after the flip is used to advantage for the study of the molecular order present. A more elaborate description of these measurements can be found in ref 10. The NMR-based orientation values are in very good agreement with the ones obtained by the FTIR measurements as can be seen from the data in Table 1. Note that the orientation found in the unstretched films (stretch ratio = 1) is caused by the thermal volume reduction of the films that are fixed at both ends during the elimination process. This comment is also relevant for the FTIR data and will be discussed in more detail further on.

c. WAXD. Both cold-stretched and hot-stretched PPV films were studied using synchrotron WAXD techniques. According to ref 14, the orientation of a crystallographic plane can be extracted from an azimuthal scan through a suitable diffraction peak at a fixed 2θ scattering angle using eq 2

$$f_{hkl} = \frac{1}{2}(3\langle\cos^2\phi_{hkl}\rangle - 1) \tag{2}$$

with

$$\langle\cos^2\phi_{hkl}\rangle = \frac{\int_0^{\pi/2} I(\phi)\sin\phi\cos^2\phi\,\mathrm{d}\phi}{\int_0^{\pi/2} I(\phi)\sin\phi\,\mathrm{d}\phi} \tag{3}$$

where f_{hkl} is the orientation value of the normal to the *hkl* plane and $I(\phi)$ is the intensity measured at an azimuthal angle ϕ. This gives the orientation of a certain crystallographic plane, which is not necessarily the same as the orientation of the chain axis. To obtain the desired Hermans orientation value of the polymer chains, the measurement of several reflections is usually necessary and the crystal structure needs to be known. It was shown by Wilchinsky, however, that in the case of fiber symmetry (which is the case for PPV films[8]) this *f* value can be found rather easily with formula 4[15]

$$\langle\cos^2\phi_c\rangle = \frac{1 - g^2 - 2\langle\cos^2\phi_{hkl}\rangle}{1 - 3g^2} \tag{4}$$

with ϕ_c being the angle between the crystallographic *c* axis and the stretch direction and *g* being the cosine of the angle between the normal to the *hkl* plane and the crystallographic *c* axis. When considering an *hk*0 plane, *g* is by definition 0, and the desired formula for the Hermans orientation value *f* is obtained:

$$f = \frac{1}{2}(3\langle\cos^2\phi_c\rangle - 1) = 1 - 3\langle\cos^2\phi_{hk0}\rangle \tag{5}$$

Equation 5 allows us to obtain the orientation value for PPV simply by making an azimuthal scan of one single *hk*0 reflection. The strongest reflection observed in our diffraction experiments was the first equatorial reflection, which is attributed to the 110 reflection.[16] A Gauss curve was fitted through the data points, and this was used for the data analysis. The measured orientation values were in very good agreement with those reported in the literature (which were usually measured on thicker films) and were reproducible. Our measurements confirmed that the degree of orientation in the cold-stretched films is at least as good as in the hot-stretched ones and for the lower stretch ratios even better (see Table 1). The fact that the values obtained with X-ray diffraction techniques are somewhat higher than the ones obtained by FTIR is generally ascribed to the fact that the former is biased toward the more ordered (crystalline) regions whereas the latter treats both crystalline and amorphous regions in a similar way.[2]

d. Interpretation of the Observed Orientation. The orientation which is induced in a semiflexible polymer by stretch-aligning the sample is often described using the Kratky model.[11] This model assumes

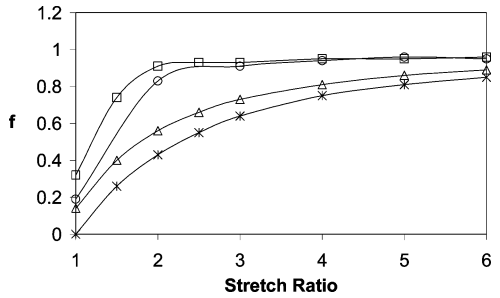

Figure 2. Hermans orientation values *f* as obtained by FTIR dichroic measurements for cold-stretched PPV (□) and hot-stretched PPV (○), as predicted by the Kratky model (∗) and as predicted by the volume-corrected Kratky model (△).

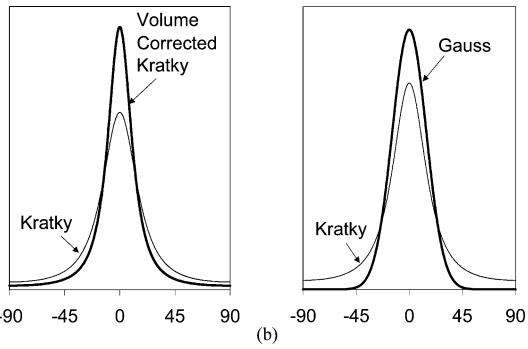

Figure 3. (a) Comparison between the angular orientation distribution function (normalized) according to the Kratky model and to the volume-corrected Kratky model (volume reduction 50%, see text) both at a stretch ratio of 2. (b) Comparison between the orientation distribution function (normalized) according to the Kratky model (stretch ratio 2) and the corresponding Gauss distribution with the same width.

that the polymer chains are rigid units, whose orientation follows the macroscopic deformation of the sample. Since effects such as viscous flow and chain relaxation are not taken into account, the predicted value usually gives an upper limit for the orientation which can be achieved by stretch alignment. Figure 2 shows the Hermans orientation values, *f*, of cold-stretched and hot-stretched PPV as obtained by the FTIR measurements as well as the predicted orientation from the Kratky model. It clearly shows that the orientation obtained is substantially higher than predicted. This difference may be due to another assumption which is made in the classic Kratky model, namely that of a constant volume of the polymer. The volume of a polymer usually *is* the same before and after stretching, but this is not the case for PPV. During the thermal conversion of the precursor to PPV the total sample volume decreases by about 50%[3] as the volatile elimination products diffuse out of the film. Because the films are held between clamps, the length of the polymer is fixed and an additional stretching process is created. The clamping of the films during the elimination makes that the effective stretch ratio for PPV polymers is actually higher than that measured. This also explains the orientation in unstretched PPV films. To account quantitatively for this effect, the Kratky model was modified by introducing a volume correction factor *b*, so that

$$V_{\text{final}} = (1/b)V_{\text{initial}} \tag{6}$$

When the Kratky model is then further derived in a similar way as described by Zbinden,[11] a volume-corrected Kratky model is obtained, and the orientation distribution function can be written as

$$a(\gamma') = \frac{b\lambda^{3/4}}{(\lambda^{-3/2}\cos^2\gamma' + b\lambda^{3/2}\sin^2\gamma')^{3/2}} \tag{7}$$

with λ being the stretch ratio, which is defined as the length of the polymer after stretching divided by its initial length. A detailed description on the origin of eq 7 can be found in the Appendix. When a volume reduction of 50% is assumed, the distribution function becomes narrower indeed, as can be seen in Figure 3. The figure shows both the Kratky distribution and the volume-corrected Kratky distribution for a film with a stretch ratio of two. Note that the overall features of the curves are almost identical, the main difference being a narrowing of the distribution when introducing the volume correction factor. From these curves, the orientation values were calculated as a function of the stretch ratio and are displayed in Figure 2. It is immediately clear that the orientation values are higher than predicted by the original Kratky model, but the difference does not suffice to explain the observed orientation in PPV. Even a volume reduction of as much as 90% would yield orientation values lower than the ones observed, so other factors need to be considered like for example the shape of the orientation distribution function.

Of the three techniques used, only FTIR does not make any assumptions on the shape of the orientation distribution function in the analysis of the data. In the case of the WAXD experiments, it was pointed out that a Gauss curve was fitted through the experimental data, and also for the data analysis of the DECODER NMR experiments, the shape of the orientation distribution function was explicitly assumed to be Gaussian. When the influence of this shape of the orientation distribution function is further analyzed, it becomes clear that its effect on the obtained orientation values can be very substantial. This is shown in Figure 3, which gives a normalized Kratky distribution for a stretch ratio of 2. From this curve, the full width at half-height was taken, and a normalized Gauss distribution with the same width was constructed. In the case of a stretch ratio of 2, there is a noticeable difference between both curves, but this difference becomes smaller at higher stretch ratios. The main difference between the two curves is the more rapid decrease toward zero intensity of the Gauss distribution as compared to the Kratky distribution. The orientation values of both distributions differ dramatically, however. For the Kratky distribution, an *f* value of 0.43 is found; for the as-constructed Gauss distribution this has risen to 0.84. This clearly demonstrates that the shape of the distribution function has a very pronounced effect on the orientation values found.

Since the FTIR measurements do not make any assumptions on the shape of this distribution and since they probe both the amorphous and crystalline regions in a similar way, we can safely assume that the orientation values obtained with this technique are correct. The fact that the values found with both WAXD and NMR, which assume a Gauss distribution, are in close to perfect agreement with these from the FTIR data strongly indicates that the shape of the distribution is very close to a Gauss curve.

These two findings can be combined to describe the orientation values found for PPV. To do so, the orientation distribution functions according to the volume-

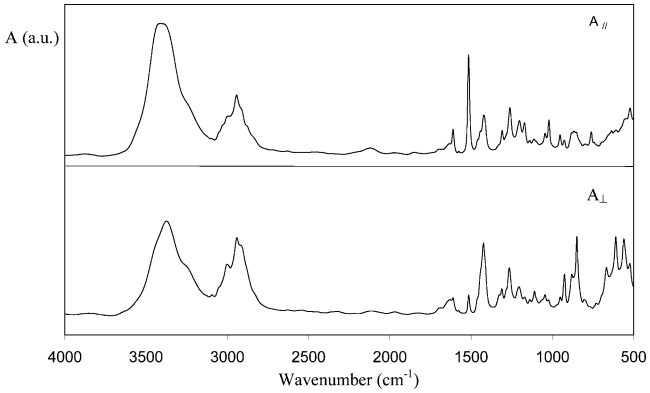

Figure 4. Polarized FTIR spectrum of a PPV precursor with a stretch ratio of 5. The spectrum recorded with the polarization parallel to the stretch direction is shown at the top and the one with the polarization perpendicular to it at the bottom.

Table 2. Comparison of the Calculated (See Text) and Observed Orientation Values *f* of PPV as a Function of the Stretch Ratio

stretch ratio	calcd *f*	obsd *f*	stretch ratio	calcd *f*	obsd *f*
1	0.24	0.32	3	0.97	0.93
1.5	0.80	0.74	4	0.99	0.95
2	0.92	0.91	5	0.99	0.95
2.5	0.95	0.93			

corrected Kratky model were calculated for several stretch ratios. A Gauss distribution was then constructed with the same full width at half-height, and the orientation value of that Gauss distribution was calculated. The results are shown in Table 2. It clearly shows that the predicted values are very similar to those observed. Although the Gaussian shape of the orientation distribution function for PPV is not conclusively proven yet, it is believed that a Gauss curve indeed gives a reasonable description of the molecular orientation present in PPV. As will be discussed in the following part on the molecular orientation in stretched precursor films, the exceptionally high degree of orientation in PPV is not solely a consequence of the elimination process. We therefore conclude that the combination of a volume-corrected Kratky model with a change in shape of the distribution function toward a Gauss distribution gives an accurate description of the orientation in PPV films.

B. Molecular Orientation in Stretched Precursor Films. a. FTIR Dichroism. Figure 4 shows the polarized IR spectra of an aligned precursor film, with a stretch ratio of 5. Although several modes show strong dichroism, only the mode at 1515 cm^{-1} is well resolved and can be used to probe the orientation. In contrast to PPV, the precursor polymer cannot be considered as a rigid and regular structure, which makes it impossible to determine the angle, α, between the transition dipole moment and the chain axis. Therefore, an exact determination of the degree of orientation in the precursor cannot be made by these FTIR measurements alone. By assuming an angle equal to 0° for the mode at 1515 cm^{-1}, a minimum orientation needed in order to be in correspondence with the observed dichroic ratio can be determined.[6] The results are shown in Table 3.

The mode at 1515 cm^{-1} can be assigned to the "semicircle" ring stretch vibration, which is also present in the spectra of PPV,[5,17,18] at 1518 cm^{-1}. Table 3 shows that the precursor has a lower dichroic ratio than PPVand that this is the case for every stretch ratio. The

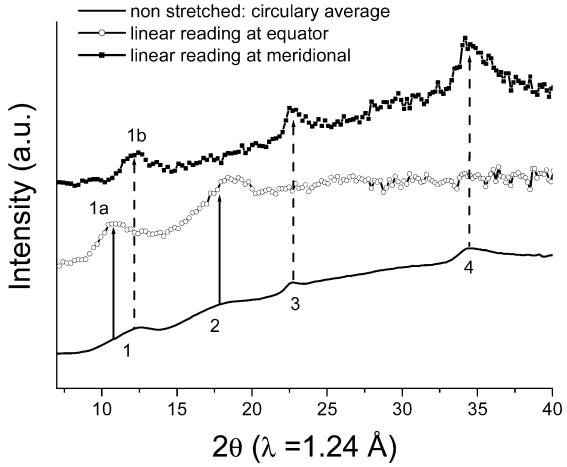

Figure 5. Scattered intensity as a function of the scattering angle obtained by circularly averaging the 2D pattern of the nonoriented precursor sample and by making linear readings along the equator or the meridional after stretching. The corresponding 2D scattering pattern of the stretched sample can be found in Figure 6 at the upper left. Labels are added to the peaks for reference in the text. The scattering patterns in this figure suffer from a considerable background, for which could not easily be corrected as explained in the experimental session.

Table 3. Dichroic Ratio, *R*, of the "Semicircle" Ring Stretch Mode of the Precursor and the Minimum (α = 0°),[6] f_{min}, and Maximum (α = 23°),[6] f_{max}, Molecular Orientation, Corresponding to the Observed Dichroic Ratio

stretch ratio	*R*	f_{min}	f_{max}
2	4.4	0.53	0.69
3	7.0	0.67	0.86
4	9.1	0.73	0.95
5	9.8	0.75	0.97
6	10.6	0.76	1.00

maximum orientation in the stretched precursor films can be found by assuming that a perfect orientation is reached for a stretch ratio of 6. From this, α was calculated to be 23°. The thus-obtained orientation values are given in Table 3. For the lower stretch ratios, it can be seen that these maximum values are still lower than the corresponding values in stretched PPV. A more detailed discussion on the FTIR linear dichroism measurements on the precursor can be found in the literature.[6]

b. X-ray Diffraction (WAXD). The exact degree of orientation present in the precursor and in PPV can be determined with X-ray diffraction measurements, using the analysis described above. A set of very weak and broad reflections was observed for the precursor in the present case prior to stretching as illustrated in Figure 5. Ezquerra et al. reported[19] two broad reflections with maxima at angles that correspond to distances of 5.88 and 4.25 Å, which in the present case with $\lambda = 1.24$ Å are found close to the expected scattering angles of 12.1° and 16.7° 2θ. They are labeled 1 and 2 in Figure 5. Here, data were collected up to higher angles and reveal the presence of two additional maxima at about 23° and 34° 2θ, labeled 3 and 4. Upon stretching, the four reflections split into two equatorial and three meridional ones, since apparently peak 1 of the nonoriented sample hides two reflections, labeled 1a and 1b. The upper left scattering pattern of Figure 6 corresponds to the precursor in a stretched state. The widths of the latter two peaks (1a and 1b) were analyzed with the Scherrer

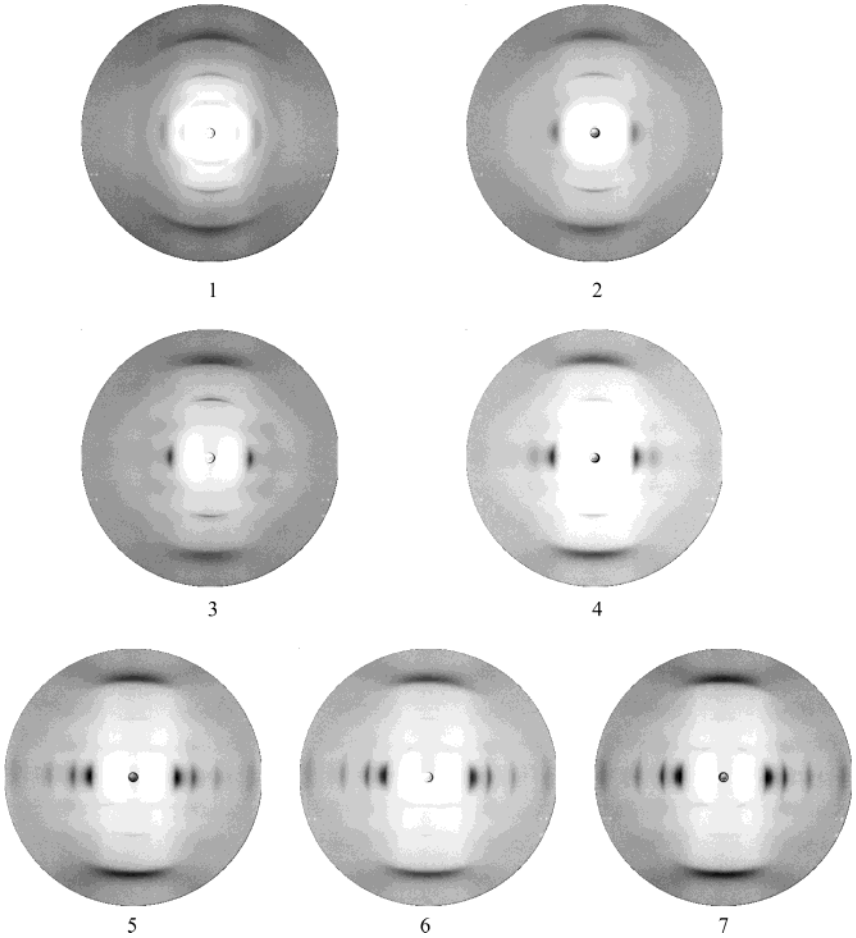

Figure 6. Diffraction patrons at seven (numbered) different stages of the elimination process, going from precursor (1) to PPV (7). For the experimental conditions, see text and Figure 7.

equation to yield a "minimum crystallite dimension" in a direction perpendicular to that of the reflecting planes and yielded values of 37 and 25 Å, respectively, corresponding to only slightly more than just next-neighbor correlation.[14] As such it is believed that this set of reflections is more compatible with a short-range ordered liquid rather than with small and highly distorted crystals, although this difference probably is mainly semantic in nature. In fact, true crystallinity is not expected for this particular sample since the tetrahydrothiophene side groups are rather bulky and there are no indications for a stereoselective synthesis. Most likely, the equatorial reflections correspond to characteristic interchain distances whereas the meridional ones correspond to distances along and perhaps within the chain. Further research is needed to elucidate the origin of these reflections.

Stretching of the precursor films was accomplished with a homemade device. Stacks of four precursor films were stretched simultaneously to improve the signal-to-noise ratio. During the stretching experiments, necking and film slippage occurred, making an exact evaluation of the orientation difficult. Therefore, another strategy was followed. A stack of four precursor films was stretched to a stretch ratio of 5, and the diffraction patterns were recorded at various stages of the elimination process. Stepwise elimination was induced by putting the same clamped set of films in an oven at increasingly higher temperatures. After each elimination step the setup was mounted again in the X-ray beam for a WAXD measurement at room temperature.

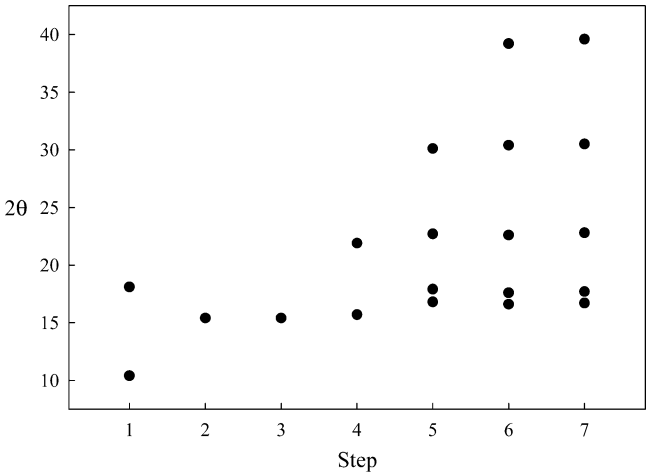

Figure 7. Angular positions of the observed equatorial reflections at the subsequent elimination steps (1, room temperature; 2, after 15 min at 100 °C; 3, after 15 min at 150 °C; 4, after 15 min at 200 °C; 5, after 15 min at 250 °C; 6, after 15 min at 300 °C; 7, after 30 min at 300 °C).

Seven steps were made of which the scattering patterns are displayed in Figure 6 (1, room temperature; 2, after 15 min at 100 °C; 3, after 15 min at 150 °C; 4, after 15 min at 200 °C; 5, after 15 min at 250 °C; 6, after 15 min at 300 °C; 7, after 30 min at 300 °C). The angular positions of the equatorial reflections are represented in Figure 7. The equatorial reflection at 3.94 Å (the peak labeled "1a" in Figure 5) gives an orientation value f of 0.743 for the stretched precursor (step 1). At the end of

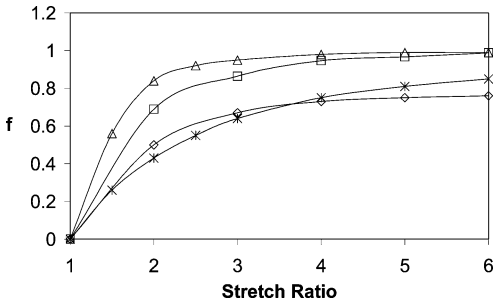

Figure 8. Orientation values *f* for the stretched precursor samples: minimal orientation from FTIR (◇), estimated orienation from FTIR and WAXD (i.e., maximum orientation, □), the Kratky model (∗), and a Gauss distribution based on the Kratky model (△).

the elimination process the value obtained from the PPV 4.29 Å reflection is $f = 0.931$. When comparing this value with the ones found for single films of cold-stretched PPV, it is noticed that the orientation is lower than expected for a stretch ratio of 5 (see Table 1). Actually, it is rather close to that of a stretch ratio of 2 or 2.5. This is most probably due to a poor grip between the stretching device and the films, and between the films mutually, resulting in film slippage. We therefore assume that the actual stretch ratio reached by the precursor stack was not 5 but 2. From the FTIR measurements on the stretched precursor films, it was found that the maximum orientation of a stretched precursor film with a stretch ratio of 2 is $f = 0.69$. This value corresponds rather well to the one obtained from the WAXS study, i.e., $f = 0.74$, keeping in mind the overestimation of the orientation by X-ray diffraction. In short, the FTIR-based f_{max} values are, according to the X-ray orientation analysis, probably the appropriate and correct ones.

c. Interpretation of the Observed Orientation. Figure 8 shows the orientation values of the stretched precursor films, obtained as described above. Probably the most striking feature of this figure is the fact that the orientation in the stretched precursor films is much higher than predicted by the Kratky model. This immediately rules out the possibility that the elimination process is the one and only factor being responsible for the unexpectedly high degrees of orientation found in PPV. Trying a similar approach as used for the stretched PPV films, the effect of a change in the shape of the orientation distribution curve toward a Gauss distribution was studied. For each stretch ratio, the (uncorrected) Kratky distribution was calculated, the width of this distribution was taken, and a Gauss distribution with the same width was constructed. The orientation parameter of that Gauss distribution was then calculated. As can be seen in Figure 8, this yields *f* values which are substantially *higher* than the ones observed.

These observations lead us to the conclusion that the unusually high orientation as observed in stretched PPV films can be attributed to three different factors: (i) a degree of orientation in the stretched precursor films which is intrinsically higher than predicted by the classic Kratky model, (ii) the introduction of extra orientation due to the volume reduction during the elimination process, and (iii) a further increase of the orientation mainly *during* the elimination reaction involving a change in shape of the orientation distribution function toward a Gauss distribution. The latter item most likely is related to PPV crystallization that happens concomitant to the elimination. The crystallization from an oriented melt occurs more readily at a given temperature essentially because this is kinetically favored. In addition, the entropy difference between crystal and oriented melt is smaller compared to that between crystal and nonoriented melt. As a result, the equilibrium melting point is increased and crystallization at a given temperature occurs more readily as it happens at a higher degree of supercooling. The stems that are added to oriented segments upon crystallization hence feed the orientation. This scenario differs from the orientation of crystals that are present *prior* to deformation for which the Kratky model was developed originally. The excess orientation in the stretched precursor film (i) is tentatively associated with ionic interactions for which some parallel chain orientation is needed. The WAXD equatorial reflections point at some preferred next-neighbor contacts. Such interactions may promote orientation. Finally, the precursor and in particular PPV have to be considered as rather stiff polymeric chains. The orientation of stiff, rodlike elements is promoted due to the associated increase of translational entropy or, more formally, the packing entropy. When the loss of orientational entropy is smaller than the gain of packing entropy, a parallel ordering can occur spontaneously as for example in the formation of liquid crystalline phases. In models by Onsager and Flory, reviewed by Fukuda et al.,[20] the packing entropy increases with the segmental axial ratio (length of the rod divided by the diameter), the polymer volume fraction, and the degree of orientation. This orientation-dependent packing effect or excluded-volume effect accounts for considerable amounts of excess orientation over that predicted in absence of such an effect.[20] Note that the polymer volume fraction increase associated with the elimination process also promotes chain orientation when thinking in terms of chains that consist of stiff rodlike segments.

4. Conclusions

The orientation in stretched precursor films and in stretched PPV films was probed using FTIR, WAXD, and DECODER NMR measurements. For both polymer systems, the observed orientation is substantially higher than predicted by the classic Kratky model. A volume-corrected Kratky model which takes into account the volume reduction during the thermal elimination process of the precursor polymer is derived, resulting in an apparently higher stretch ratio than intended, but this does not suffice to explain the observed differences. All three techniques yield very similar orientation values, although they start from different assumptions about the shape of the orientation distribution function. It is concluded that the shape of this distribution is very similar to a Gauss distribution for the PPV films, but not for the precursor films. The volume reduction and change in shape of the orientation distribution function toward a Gauss distribution during the thermal elimination reaction add to the already very high degree of orientation present in the stretched precursor films, resulting in the observed orientation values of stretch-aligned PPV films.

Acknowledgment. W.D. thanks the Fund for Scientific Research (FWO-Vlaanderen) for a grant as a research assistant. Financial support for T.V.d.K., through a Concerted Research Project of the Special

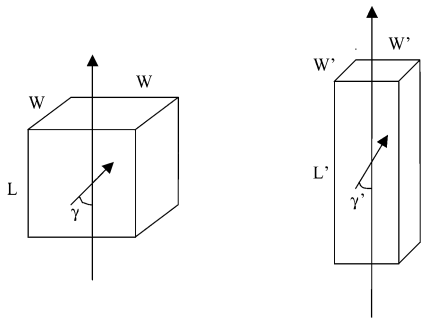

Figure 9. Correlation between macroscopic (block) and molecular (vertical arrow) deformation of a polymer sample before (left) and after (right) stretching.

Fund for Research of the University of Antwerp, is gratefully acknowledged. B.G., who currently is a postdoctoral fellow of the FWO-Vlaanderen, thanks the Research Council of the Catholic University of Leuven for a BOF research grant. The authors thank D. Schaefer for the interesting discussions and Prof. H. Reynaers and the FWO-Vlaanderen for supporting DUBBLE at the ESRF.

Appendix: Deriving the Volume-Corrected Kratky Model

The derivation of the volume-corrected Kratky model is similar to that of the classic Kratky model as described by Zbinden.[11] The distribution function $a(\gamma')$ is defined as the number of chains whose chain axis make an angle γ' with the stretch direction after the sample has been stretched form an initial length L to a final length L'. This is shown in Figure 9. The stretch ratio λ is defined as

$$\lambda = \frac{L'}{L} \tag{A1}$$

Whereas the classic Kratky model assumes a constant volume before and after stretching, we introduce a volume correction factor b.

$$W^2 L = bW'^2 L' \tag{A2}$$

Assuming that the molecular orientation of a chain segment corresponds to the macroscopic deformation of the sample, $\tan\gamma'$ is calculated.

$$\tan\gamma' = \frac{W'}{L'} \tag{A3}$$

$$\tan\gamma' = \frac{1}{L'}\sqrt{\frac{W^2 L}{bL'}} \tag{A4}$$

$$\tan\gamma' = \frac{\lambda^{-3/2}}{\sqrt{b}}\tan\gamma \tag{A5}$$

Deriving $\tan\gamma$ gives the following:

$$\mathrm{d}(\tan\gamma') = \mathrm{d}\left(\tan\gamma\,\frac{\lambda^{-3/2}}{\sqrt{b}}\right) \tag{A6}$$

$$\frac{1}{\cos^2\gamma'}\,\mathrm{d}\gamma' = \frac{\lambda^{-3/2}}{\sqrt{b}\cos^2\gamma}\mathrm{d}\gamma \tag{A7}$$

$$\frac{\mathrm{d}\gamma'}{\mathrm{d}\gamma} = \frac{\cos^2\gamma'}{\cos^2\gamma}\frac{\lambda^{-3/2}}{\sqrt{b}} = \frac{\tan^2\gamma + 1}{\tan^2\gamma' + 1}\frac{\lambda^{-3/2}}{\sqrt{b}} = \frac{\tan^2\gamma + 1}{\frac{\lambda^{-3}}{b}\tan^2\gamma + 1}\frac{\lambda^{-3/2}}{\sqrt{b}} \tag{A8}$$

Now, the number of chain segments in the interval γ to $\gamma + \mathrm{d}\gamma$ is equal to $a(\gamma)\sin\gamma$ (see Zbinden). The same chain segments point into the interval γ' to $\gamma' + \mathrm{d}\gamma'$.

$$a(\gamma)\sin\gamma\,\mathrm{d}\gamma = a(\gamma')\sin\gamma'\,\mathrm{d}\gamma' \tag{A9}$$

Finally, the formula for $a(\gamma')$ is calculated. $a(\gamma) = 1$ by definition for a random distribution. Using eq A9, we get

$$a(\gamma')\sin\gamma' = \sin\gamma\,\frac{\mathrm{d}\gamma}{\mathrm{d}\gamma'} \tag{A10}$$

$$a(\gamma')\sin\gamma' = \frac{\sin\gamma\sqrt{b}}{\lambda^{-3/2}}\frac{\frac{\lambda^{-3}}{b}\tan^2\gamma + 1}{\tan^2\gamma + 1} = \lambda^{3/2}\sqrt{b}\sin\gamma\,\frac{\tan^2\gamma' + 1}{b\lambda^3\tan^2\gamma' + 1} \tag{A11}$$

$$= \frac{\lambda^{3/2}\sin\gamma\sqrt{b}}{b\lambda^3\sin^2\gamma' + \cos^2\gamma'} \tag{A12}$$

with

$$\frac{1}{\sin\alpha} = \sqrt{\frac{1}{\tan^2\alpha} + 1} \tag{A13}$$

Formula A12 gives

$$a(\gamma')\sin\gamma' = \frac{\lambda^{3/2}\sqrt{b}}{b\lambda^3\sin^2\gamma' + \cos^2\gamma'}\frac{1}{\sqrt{\frac{1}{\tan^2\gamma} + 1}} = \frac{\lambda^{3/2}\sqrt{b}}{b\lambda^3\sin^2\gamma' + \cos^2\gamma'}\frac{1}{\sqrt{\frac{\lambda^{-3}}{b\tan^2\gamma'} + 1}} \tag{A14}$$

Transforming formula A14 leads to

$$a(\gamma')\sin\gamma' = \frac{\lambda^{3/2}\sqrt{b}}{b\lambda^3\sin^2\gamma' + \cos^2\gamma'}\frac{\sqrt{b}\sin\gamma'}{\sqrt{\lambda^{-3}\cos^2\gamma' + b\sin^2\gamma'}} = \frac{b\lambda^{3/4}\sin\gamma'}{(\lambda^{-3/2}\cos^2\gamma' + b\lambda^{3/2}\sin^2\gamma')^{3/2}} \tag{A15}$$

Eliminating $\sin\gamma'$ at both sides eventually gives the modified Kratky formula

$$a(\gamma') = \frac{b\lambda^{3/4}}{(\lambda^{-3/2}\cos^2\gamma' + b\lambda^{3/2}\sin^2\gamma')^{3/2}} \tag{A16}$$

References and Notes

(1) Gagnon, D. R.; Karasz, F. E.; Thomas, E. L.; Lenz, R. W. *Synth. Met.* **1987**, *20*, 85−95.
(2) Lenz, R. W.; Han, C. C.; Stengersmith, J. D.; Karasz, F. E. *J. Polym. Sci., Polym. Chem.* **1988**, *26*, 3241−3249.

(3) Machado, J. M.; Karasz, F. E.; Kovar, R. F.; Burnett, J. M.; Druy, M. A. *New Polym. Mater.* **1989**, *1*, 189−207.
(4) Machado, J. M.; Masse, M. A.; Karasz, F. E. *Polymer* **1989**, *30*, 1992−1996.
(5) Dermaut, W.; Van den Kerkhof, T.; van der Veken, B. J.; Mertens, R.; Geise, H. J. *Macromolecules* **2000**, *33*, 5634−5637.
(6) Dermaut, W.; Van den Kerkhof, T.; Zhang, X. B.; van der Veken, B. J.; Mertens, R.; Geise, H. J. *Synth. Met.* **2001**, *119*, 295−296.
(7) Gregorius, R.; Karasz, F. E. *Eur. Polym. J.* **1993**, *29*, 159−162.
(8) Zhang, X. B.; Van Tendeloo, G.; Van Landuyt, J.; Van Dyck, D.; Briers, J.; Bao, Y.; Geise, H. J. *Macromolecules* **1996**, *29*, 1554−1561.
(9) Bradley, D. D. C.; Friend, R. H.; Lindenberger, H.; Roth, S. *Polymer* **1986**, *27*, 1709−1713.
(10) Kropewnicki, M.; Schaefer, D.; Dermaut, W.; Geise, H. J. Chmelka, B. F. *Solid State Nucl. Magn. Reson.* **2002**, *22*, 275−297.
(11) Zbinden, R. In *Infrared Spectroscopy of High Polymers*; Academic Press: New York, 1964.
(12) Schmidtrohr, K.; Hehn, M.; Schaefer, D.; Spiess, H. W. *J. Chem. Phys.* **1992**, *97*, 2247−2262.
(13) Chmelka, B. F.; Schmidtrohr, K.; Spiess, H. W. *Macromolecules* **1993**, *26*, 2282−2296.
(14) Alexander, L. E. In *X-ray Diffraction Methods in Polymer Science*; Robert E. Krieger Publishing Co.: Huntington, NY, 1979.
(15) Wilchinsky, Z. W. *Adv. X-ray Anal.* **1963**, *6*, 231−241.
(16) Granier, T.; Thomas, E. L.; Gagnon, D. R.; Karasz, F. E.; Lenz, R. W. *J. Polym. Sci., Polym. Phys.* **1986**, *24*, 2793−2804.
(17) Shah, H. V.; Manning, C. J.; Arbuckle, G. A. *Appl. Spectrosc.* **1999**, *53*, 1542−1550.
(18) Bradley, D. D. C. *J. Phys. D: Appl. Phys.* **1987**, *20*, 1389−1410.
(19) Ezquerra, T. A.; Lopez-Cabarcos, E.; Balta-Calleja, F. J.; Stenger-Smith, J. D.; Lentz, R. W. *Polymer* **1991**, *32*, 781−785.
(20) Fukuda, T.; Takada, A.; Miyamoto, T. *Macromolecules* **1991**, *24*, 6210−6214.

MA034404Y